Aaij, R. et al. (2014) Effective lifetime measurements in the B0s → K +K −, B0 → K +π− and B0s → π+K − decays. Physics Letters B, 736, pp. 446-454.

Version: Published

http://eprints.gla.ac.uk/106877

Deposited on: 01 June 2015

Contents lists available at ScienceDirect

Physics Letters B

PHYSICS LETTERS B
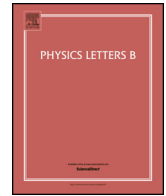
Effective lifetime measurements in the $B_s^0 \to K^+K^-$, $B^0 \to K^+\pi^-$ and $B_s^0 \to \pi^+K^-$ decays

CrossMark

LHCb Collaboration

ABSTRACT

Measurements of the effective lifetimes in the $B_s^0 \to K^+K^-$, $B^0 \to K^+\pi^-$ and $B_s^0 \to \pi^+K^-$ decays are presented using 1.0 fb^{-1} of pp collision data collected at a centre-of-mass energy of 7 TeV by the LHCb experiment. The analysis uses a data-driven approach to correct for the decay time acceptance. The measured effective lifetimes are

$$\tau_{B_s^0 \to K^+K^-} = 1.407 \pm 0.016 \,(\text{stat}) \pm 0.007 \,(\text{syst}) \text{ ps},$$

$$\tau_{B^0 \to K^+\pi^-} = 1.524 \pm 0.011 \,(\text{stat}) \pm 0.004 \,(\text{syst}) \text{ ps},$$

$$\tau_{B_s^0 \to \pi^+K^-} = 1.60 \pm 0.06 \,(\text{stat}) \pm 0.01 \,(\text{syst}) \text{ ps}.$$

This is the most precise determination to date of the effective lifetime in the $B_s^0 \to K^+K^-$ decay and provides constraints on contributions from physics beyond the Standard Model to the B_s^0 mixing phase and the width difference $\Delta\Gamma_s$.

1. Introduction

The study of $B_{(s)}^0$ mesons from the charmless $B_{(s)}^0 \to h^+h'^-$ decay family,[1] where $h^{()}$ is either a pion or a kaon, offers unique opportunities to investigate the heavy flavour sector. These decays are sensitive to charge parity (CP) symmetry violation, which allows the phase structure of the Cabibbo–Kobayashi–Maskawa (CKM) matrix [1,2] to be studied, and to manifestations of physics beyond the Standard Model (SM). The $B_{(s)}^0 \to h^+h'^-$ decays have been analysed in detail by LHCb, with measurements of the branching fractions [3], time-integrated [4] and time-dependent [5] CP violation being made. The effective $B_s^0 \to K^+K^-$ lifetime has previously been measured by LHCb using data recorded in 2010 [6] and 2011 [7], corresponding to an integrated luminosity of 37 pb^{-1} and 1.0 fb^{-1} respectively. In this paper we reanalyse the 2011 data using a data driven method that employs the full statistical power of the data set.

The detailed formalism of the effective lifetime in $B_{(s)}^0 \to h^+h'^-$ decays can be found in Refs. [8] and [9]. The decay time distribution of a $B_{(s)}^0 \to h^+h'^-$ decay, with equal contributions of both $B_{(s)}^0$ and $\overline{B}_{(s)}^0$ at the production stage, can be written as

$$\Gamma(t) \propto (1 - \mathcal{A}_{\Delta\Gamma_{(s)}})e^{-\Gamma_{\text{L}}^{(s)}t} + (1 + \mathcal{A}_{\Delta\Gamma_{(s)}})e^{-\Gamma_{\text{H}}^{(s)}t}, \qquad (1)$$

where $\Gamma_{\text{H}}^{(s)} = \Gamma_{(s)} - \Delta\Gamma_{(s)}/2$ and $\Gamma_{\text{L}}^{(s)} = \Gamma_{(s)} + \Delta\Gamma_{(s)}/2$ are the decay widths of the heavy and light mass eigenstates, $\Gamma_{(s)}$ is the average decay width and $\Delta\Gamma_{(s)}$ is the decay width difference between the mass eigenstates. These in turn are given as linear combinations of the two flavour states with complex coefficients q and p. The formalism used herein is only valid if $|q/p| = 1$.

The parameter $\mathcal{A}_{\Delta\Gamma_{(s)}}$ is defined as $\mathcal{A}_{\Delta\Gamma_{(s)}} \equiv -2\text{Re}(\lambda)/(1 + |\lambda|^2)$, where $\lambda \equiv (q/p)(\overline{A}/A)$ and A ($\overline{A}$) is the amplitude for $B_{(s)}^0$ ($\overline{B}_{(s)}^0$) decays to the respective final states. For B^0 mesons, $\Delta\Gamma$ is sufficiently small that the heavy and light mass eigenstates cannot be resolved experimentally, thus only a single exponential distribution is measured. For B_s^0 mesons, $\Delta\Gamma_s$ is large enough for the mass eigenstates to be distinguishable. This implies that fitting a single exponential distribution will yield a different *effective* lifetime when measured in different B_s^0 channels, depending on the relative proportions of the heavy and light contributions in that decay. Equal proportions of heavy and light eigenstates contribute to the $B_s^0 \to \pi^+K^-$ decay at $t = 0$, which allows measuring the flavour-specific effective lifetime. The B_s^0 flavour-specific effective lifetime can be approximated to second order by

$$\tau_{B_s^0} \approx \frac{1}{\Gamma_s} \frac{1 + (\frac{\Delta\Gamma_s}{2\Gamma_s})^2}{1 - (\frac{\Delta\Gamma_s}{2\Gamma_s})^2}. \qquad (2)$$

The $B_s^0 \to K^+K^-$ decay is treated slightly differently as the SM predicts the initial state to consist almost entirely of the light mass

---

[1] The inclusion of charge-conjugate processes is implied.

eigenstate. This can be described by stating that in the absence of CP violation the parameter $\mathcal{A}_{\Delta\Gamma_s}(B_s^0 \to K^+K^-) = -1$, thus the decay time distribution involves only the first term in Eq. (1). For small deviations from the CP-conserving limit, the distribution can be approximated to first order in $\Delta\Gamma_s/\Gamma_s$ by a single exponential with an effective lifetime

$$\tau_{B_s^0 \to K^+K^-} \approx \frac{1}{\Gamma_s}\left(1 + \frac{\mathcal{A}_{\Delta\Gamma_s}\Delta\Gamma_s}{2\Gamma_s}\right). \tag{3}$$

An effective lifetime measurement in the decay channel $B_s^0 \to K^+K^-$ is of considerable interest, as it can be used to constrain the contributions from new physical phenomena entering the B_s^0 meson system [10,11,8,9,12]. This decay channel has contributions from loop diagrams that in the SM have the same phase as the B_s^0–$\bar{B}_s^0$ mixing amplitude, hence the measured effective lifetime is expected to be close to $1/\Gamma_L^s$. However, the tree contribution to the $B_s^0 \to K^+K^-$ decay amplitude introduces a small amount of CP violation. Taking the SM prediction for $\mathcal{A}_{\Delta\Gamma_s}(B_s^0 \to K^+K^-) = -0.972^{+0.014}_{-0.009}$ [8] and the measured values of Γ_s and $\Delta\Gamma_s$ from Ref. [13], the prediction for the effective $B_s^0 \to K^+K^-$ lifetime from Eq. (3) is $\tau_{B_s^0 \to K^+K^-} = 1.395 \pm 0.020$ ps.

The measurement is performed using a pp collision data sample corresponding to an integrated luminosity of 1.0 fb^{-1}, collected by the LHCb experiment at a centre of mass energy of $\sqrt{s} = 7$ TeV in 2011. A key aspect of the analysis is the correction of decay time biasing effects, referred to as the acceptance, which are introduced by the selection criteria used to maximise the signal significance of the B meson sample. A data-driven approach, discussed in detail in Ref. [14], and applied to a previous measurement of this channel [6], is used to correct for this bias.

2. Detector and data sample

The LHCb detector [15] is a single-arm forward spectrometer covering the pseudorapidity range $2 < \eta < 5$, designed for the study of particles containing b or c quarks. The detector includes a high-precision tracking system consisting of a silicon-strip vertex detector (VELO) surrounding the pp interaction region [16] and several dedicated tracking planes with silicon microstrip detectors (Inner Tracker) covering the region with high charged particle multiplicity and straw tube detectors (Outer Tracker) for the region with lower occupancy. The Inner and Outer Tracker are placed downstream of the magnets to allow the measurement of the charged particles momenta as they traverse the detector. Excellent particle identification (PID) capabilities are provided by two ring-imaging Cherenkov detectors, which allow charged pions, kaons, and protons to be distinguished from each other in the momentum range 2–100 GeV/c [17]. The experiment employs a multi-level trigger to reduce the readout rate and enhance signal purity: a hardware trigger based on the measurement of the transverse energy deposited in the calorimeter cells and the momentum transverse to the beamline (p_T) of muon candidates, as well as a software trigger that allows the reconstruction of the full event information.

The average momentum of the produced B mesons is around 100 GeV/c and their decay vertices are displaced from the primary interaction vertex (PV). Background particles in general have low momentum and originate from the primary pp collision. The candidates used in this analysis are reconstructed from events selected by the hardware trigger containing large hadronic energy depositions and originating from the signal particles, or events selected independently of the signal particles. The signal sample is further enriched by the software-based trigger with an exclusive selection on $B_{(s)}^0 \to h^+h'^-$ candidates.

The offline selection is based on a cut-based method, which is designed to maximise the signal significance. The selection requires that the tracks associated with the B meson decay products have a good track fit quality per number of degrees of freedom, $\chi^2/\text{ndf} < 3.3$. The transverse momentum of at least one particle from the decay is required to have $p_T > 2.5$ GeV/c, with the other having $p_T > 1.1$ GeV/c. Each decay product must also have a large χ^2_{IP}, defined as the difference in χ^2 of the primary pp interaction vertex reconstructed with and without the considered particle. The minimum value of the χ^2_{IP} of the two decay products is required to be greater than 45, and the larger of the two greater than 70.

The B meson candidate is obtained by reconstructing the vertex formed by the two particles. It is required to have $\chi^2_{\text{IP}} < 9$ and a reconstructed decay time greater than 0.6 ps. Each pp interaction vertex in an event is fitted with both the reconstructed charged particles, where there are typically 1.7 interaction vertices per bunch crossing. The angle between the direction of flight from the best PV to decay vertex, and the B momentum vector, must be smaller than 19 mrad. The best PV is defined as the PV to which the B candidate has the lowest χ^2_{IP} value.

The final selection of the $B_{(s)}^0 \to h^+h'^-$ modes is performed by identifying pions, kaons and protons using PID likelihood observables obtained from the ring-imaging Cherenkov detectors [17]. Simulated samples of these $B_{(s)}^0 \to h^+h'^-$ modes are also generated for verification. In the simulation, pp collisions are generated using PYTHIA [18] with a specific LHCb configuration [19]. Decays of hadronic particles are described by EvtGen [20], in which final state radiation is generated using Photos [21]. The interaction of the generated particles with the detector and its response are implemented using the Geant4 toolkit [22] as described in Ref. [23].

3. $B_{(s)}^0 \to h^+h'^-$ lifetime measurements

The reconstructed $B_{(s)}^0 \to h^+h'^-$ mass and lifetime spectra include many contributions in addition to the combinatorial background, which arises from random combinations of reconstructed tracks. These backgrounds must be modelled accurately to reduce potential biases in the final measurement. The additional backgrounds consist of misreconstructed multi-body decays and misidentified physics backgrounds. Multi-body decays, such as the process $B^0 \to K^+\pi^-\pi^0$, may be reconstructed incorrectly as two body decays and in general populate a region of lower values than the signal in the mass spectrum. Misidentified backgrounds may originate from other $B_{(s)}^0 \to h^+h'^-$ decays due to misidentification of the final state particles, where the correctly identified $B^0 \to K^+K^-$ is treated as a misidentified background in the fit to the K^+K^- spectrum. The $B^0 \to K^+K^-$ decay is treated this way due to its relative contribution being too small to fit for using a parametrised function.

The effective $B_{(s)}^0 \to h^+h'^-$ lifetimes are extracted using an unbinned maximum likelihood fit in which probability density functions (PDFs) are used to describe the mass and decay time distributions. The measurement is performed by factorising the process into two independent fits, where the mass and decay time have been verified to be uncorrelated by correlation plots and comparing the decay time distribution in different mass intervals for the combinatorial background. The first fit is performed to the observed mass spectrum, see Fig. 1, and is used to determine the signal and background probabilities of each candidate. The yield of each misidentified background is fixed to the yield of the primary signal peak, $B_s^0 \to K^+K^-$ or $B^0 \to K^+\pi^-$, using the world average branching fractions and measured hadronisation ratios [24]. The deviation visible around the $B^0 \to K^+K^-$ peak in the $B_s^0 \to K^+K^-$ mass fit, Fig. 1 (left), may be due to limited knowledge of the
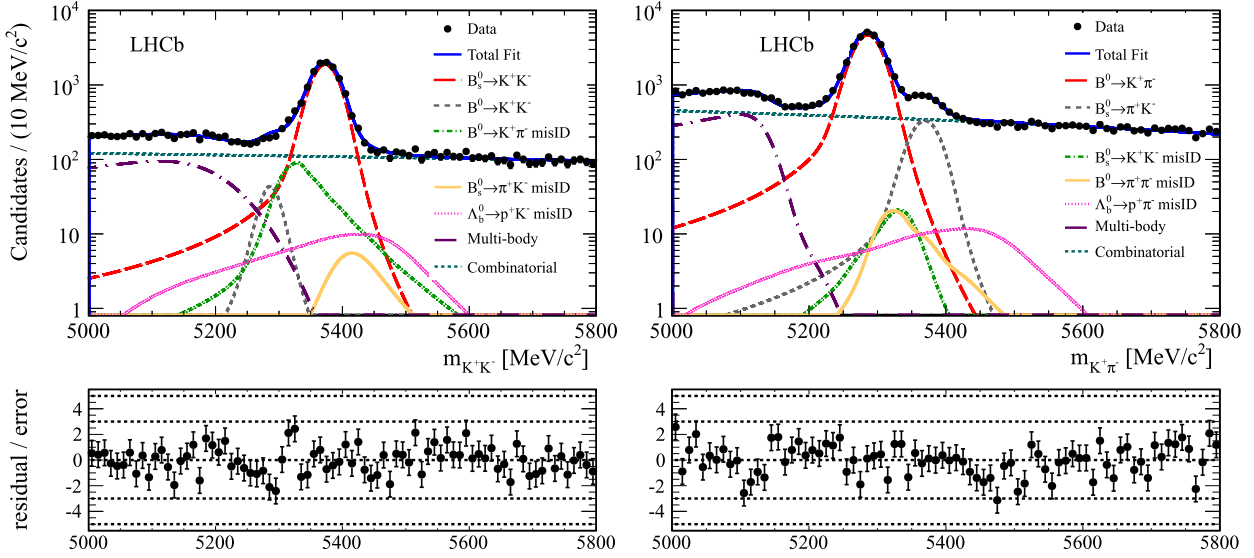
Fig. 1. Fits to the (left) K^+K^- and (right) $K^+\pi^-$ invariant mass spectrum, with the main contributory signal and background components displayed. The fit residuals are provided beneath each respective mass spectra.

$B^0 \rightarrow K^+K^-$ branching fraction. The mass fit probability density $f(m)$ can be written as the sum over the individual PDFs, $f(m|\text{class})$, for all signal and background classes multiplied by the corresponding relative yield of that class $P(\text{class})$,

$$f(m) = \sum_{\text{class}} f(m|\text{class}) \cdot P(\text{class}), \qquad (4)$$

where m is the measured mass of the candidate. The PDF models used to describe the mass distributions of each class are determined from full LHCb simulation, with the exception of the multi-body background in the K^+K^- spectrum that uses both simulation and data for its description. A sum of two Crystal Ball (CB) functions [25] describes the $B_s^0 \rightarrow K^+K^-$, $B^0 \rightarrow K^+\pi^-$ and $B_s^0 \rightarrow \pi^+K^-$ signal decays. Misidentified background classes are described by template models extracted from simulation. The multi-body background is described using an exponentially modified Gaussian distribution,[2] while the combinatorial background component is modelled with a first order polynomial. Only candidates in the mass range 5000–5800 MeV/c^2 are used, with 22 498 and 60 596 candidates contributing to the K^+K^- and $K^+\pi^-$ spectrum, respectively. The fits to each invariant mass spectrum yield $10\,471 \pm 121$ $B_s^0 \rightarrow K^+K^-$, $26\,220 \pm 200$ $B^0 \rightarrow K^+\pi^-$ and 1891 ± 85 $B_s^0 \rightarrow \pi^+K^-$ signal events. In addition, the *sWeights* [26], signal fractions $P(\text{class})$ and the probability of an event belonging to a particular signal class are also calculated by the mass fit and are used in the subsequent lifetime fit.

A fit to the reconstructed decay time spectrum is performed to measure the effective lifetime. The spectrum is described by a single exponential function, using a per-event acceptance correction calculated from data. The method used to evaluate the acceptance correction is detailed in Refs. [14,6]. The per-event acceptance functions are determined by moving each primary vertex along the momentum vector of the corresponding B particle, and re-evaluating the selection for each emulated decay time. This procedure is repeated for a large number of hypothetical PV positions to verify whether a candidate would have been selected at that decay time. The set of decay times at which the per-event acceptance function turns on and off is denoted by A in Eq. (5). The decay

time PDF is modelled using a description of the unbiased distribution multiplied by the per-event acceptance function, denoted by $f(t|A, \text{class})$. The likelihood function per candidate is given by

$$f(t, A|m)$$
$$= \sum_{\text{classes}} f(t|A, \text{class}) \cdot f(A|\text{class}) \cdot \frac{P(\text{class}) f(m|\text{class})}{f(m)}, \qquad (5)$$

where t is the reconstructed decay time and $f(A|\text{class})$ is the observed distribution of A determined by the *sPlot* technique. The last factor is the probability for the candidate to belong to a particular signal class.

The decay time PDFs of the background classes are modelled differently from the signal. The misidentified $B_{(s)}^0 \rightarrow h^+h'^-$ backgrounds are described using an exponential function, with each lifetime fixed to the respective current world average [27]. This is an approximation as these decays are reconstructed under the wrong mass hypothesis and a systematic uncertainty is assigned in Section 4. The decay time PDFs of both the multi-body and combinatorial background are estimated from data using a non-parametric method involving the sum of kernel functions [28]. These functions represent each candidate with a Gaussian function centred at the measured decay time, with a width related to an estimate of density of candidates at this decay time [28] and normalised by the *sWeight* [26] of the candidate. The density of candidates is estimated by the *sPlot* [29] of the decay time distribution for each signal class.

This procedure approximates the observed decay time distribution, including the acceptance effects. The fit method requires unbiased decay time distributions since these are multiplied by the per-event acceptance functions. The unbiased distributions are calculated from the estimated observed distribution divided by the average acceptance functions. The average acceptance function is calculated from an appropriately weighted sum of the per-event acceptance functions.

The lifetime fit is performed in the decay-time range 0.61–10.00 ps, due to a decay time cut of 0.60 ps in the selection and to ensure that a sufficiently large number of candidates is available for the method to be stable. The fit results for the $B_{(s)}^0 \rightarrow h^+h'^-$ channels are displayed in Fig. 2.

---

[2] $f(m; \mu, \sigma, \lambda) = \frac{\lambda}{2} e^{\frac{\lambda}{2}(2\mu + \lambda\sigma^2 - 2m)} \text{erfc}(\frac{\mu + \lambda\sigma^2 - m}{\sqrt{2}\sigma})$.
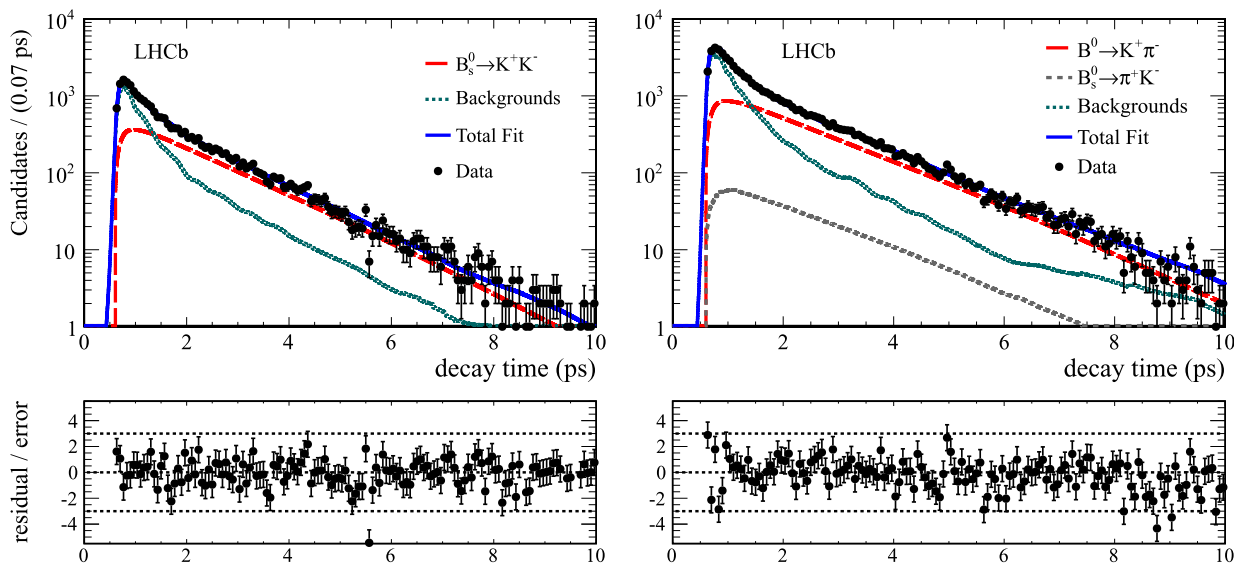
Fig. 2. Fit to the reconstructed decay times of the (left) $B_s^0 \to K^+K^-$ decay and simultaneous fit to the (right) $B^0 \to K^+\pi^-$ and $B_s^0 \to \pi^+K^-$ reconstructed decay times. The background distribution is the sum of all backgrounds displayed in Fig. 1. The fit residuals are provided beneath each respective decay time spectra.

Table 1
Systematic uncertainties on the effective lifetimes. The uncertainties vary between the $B_s^0 \to K^+K^-$, $B^0 \to K^+\pi^-$ and $B_s^0 \to \pi^+K^-$ measurements due to the available sample size per decay mode.

Source	Uncertainty (fs)		
	$B_s^0 \to K^+K^-$	$B^0 \to K^+\pi^-$	$B_s^0 \to \pi^+K^-$
Cross contamination	4.8	1.3	6.0
Tracking efficiency	2.8	2.8	2.8
Mass model	1.1	2.5	6.7
B_c^+ contamination	1.1	–	1.1
Non-parametric decay time modelling	0.8	1.6	6.7
Production asymmetry	3.0	–	–
Effective lifetime interpretation	1.2	–	–
Remaining uncertainties	0.8	0.6	3.7
Total	6.7	4.3	12.2

4. Systematic studies

The systematic uncertainties are listed in Table 1 and discussed below.

The dominant contribution to the systematic uncertainty, in particular for the $B_s^0 \to K^+K^-$ and $B_s^0 \to \pi^+K^-$ effective lifetimes, comes from the contamination from misidentified $B_{(s)}^0 \to h^+h'^-$ background channels. To determine the relative contribution of the most significant misidentified backgrounds, we first determine the misidentification probability of protons, pions and kaons as measured in data using the decays $K_S^0 \to \pi^+\pi^-$, $D^0 \to K^-\pi^+$, $\phi \to K^+K^-$ and $\Lambda \to p\pi^-$, where the particle type is deduced without using PID information. The particle identification likelihood method used to separate pions, kaons and protons depends on kinematic and global event information such as momentum, transverse momentum, and the number of reconstructed primary interaction vertices. The events in the calibration samples are weighted to match the distributions of these variables in the signal sample. The mass spectrum of the misidentified backgrounds are fitted under the correct mass hypothesis to extract the yields, before being translated into cross-contamination rates using the PID efficiencies and misidentification rates. For the sub-dominant backgrounds, the known branching and hadronisation fractions are used to estimate the yields instead of the fitted values. The value of the systematic uncertainty is given by the change in the fitted lifetime when the contamination rates are varied within their uncertainty.

Another systematic uncertainty arises from the track reconstruction efficiency and applies equally to all three decays. The track finding algorithm prefers tracks originating from the beamline, so those from long-lived B decays have a slightly lower reconstruction efficiency. To determine the impact of this uncertainty, the track reconstruction efficiency is parametrised from data and then emulated in a large number of simulated pseudoexperiments. Further details about this effect, and its parametrisation, are provided in Ref. [30]. The difference between the generated and fitted lifetimes is determined and the full offset is subtracted from the final fitted lifetime and 50% of the value is assigned as a systematic uncertainty.

The sensitivity to the details of the implemented signal and background mass models are studied by varying the model parameters taken from simulation. This systematic uncertainty particularly affects the effective lifetime in the $B_s^0 \to \pi^+K^-$ decay. The tail parameters of the double Crystal Ball function describing the signal peaks and the parameters of the exponentially modified Gaussian function describing the multi-body backgrounds are varied to accommodate the differences between simulations and data.

The position of the mass shapes of the misidentified backgrounds are fixed relative to the position of the signal peaks. The offset is varied from the central value by the uncertainty of the mean of the fitted primary signal peak to determine the effect on the fitted lifetime.

The sensitivity to the shape of the combinatorial background model is estimated by changing the description from a first-order polynomial to an exponential function, the uncertainty being given by the lifetime difference observed.

The effective lifetimes in the $B_s^0 \to K^+K^-$ and $B_s^0 \to \pi^+K^-$ decays are also affected by contamination from secondary B_s^0 mesons decaying from B_c^+ mesons. Studies of the $B_c^+ \to B_s^0 \pi^+$ decay give an upper limit of 1% on the fraction of B_s^0 mesons that originate from B_c^+ decays [31]. The systematic uncertainty is estimated from simulated pseudoexperiments, by adding a lifetime contribution that represents the B_c^+ decays with the resultant deviation from the expected lifetime assigned as the uncertainty.

The sensitivity to the modelling of the non-parametric component of the background, which comprises the multi-body and combinatorial backgrounds, is tested using three approaches. The first is estimated by varying the width of the Gaussian kernels [28] to determine their effect on the background decay time distributions. The second is studied by varying the decay time depending on the mass of the combinatorial background. This is performed by splitting the mass range 5480–5880 MeV/c^2 into three bins and ensuring that the decay time distribution in each bin shows no variation within its statistical uncertainty. The final study estimates the systematic uncertainty assuming a correlation between the decay time distribution and the mass of the multi-body and misidentified backgrounds. This is performed using simulated pseudoexperiments, where the generated lifetime is scaled by a factor determined by the ratio of the generated misreconstructed mass and the true mass for each event. The modelling of the non-parametric background has the largest influence on the effective lifetime in the $B_s^0 \to \pi^+K^-$ decay since the signal significance is the smallest in this channel.

The analysis assumes that B_s^0 and $\bar{B}_s^0$ mesons are produced in equal quantities. Deviations from this assumption affect the effective lifetime in the $B_s^0 \to K^+K^-$ decay but not the effective lifetimes in the flavour specific decays. The production asymmetry is measured experimentally to be (7 ± 5)% [5], and its influence is evaluated from an analytical calculation using the current experimental values.

This analysis presents a measurement of the effective $B_s^0 \to K^+K^-$ lifetime, which is equivalent to measuring the decay time using a single exponential function and is commonly evaluated using the formula described in Ref. [32]. This is only valid in the absence of acceptance effects. The a priori unknown fractional components of the light and heavy mass eigenstates that contribute to the decay of the B_s^0 meson result in an interpretation bias. Using conservative choices for $\Delta \Gamma_s$ and $\mathcal{A}_{\Delta \Gamma_s}$, the size of the effect is studied with simulated pseudoexperiments. The result is labelled "Effective lifetime interpretation" in Table 1 and is treated as a source of systematic uncertainty on the measurement.

The remaining sources of uncertainty are the following: the precision at which the fitting method was verified; the uncertainty on the world average lifetimes used to model the misidentified $B_{(s)}^0 \to h^+h'^-$ backgrounds; the modelling of the decay time resolution in the lifetime fit; the absolute lifetime scale given by the alignment and the absolute length of the VELO. These are all individually small and sum up to the last line in Table 1.

The method itself is verified as being unbiased using simulation of the LHCb experiment and a large number of simulated pseudoexperiments.

Additionally, studies of the effect of the trigger, primary vertices and magnet polarity are performed. The data are divided into subsets corresponding to periods with different magnet polarity, trigger configuration, and for different numbers of primary vertices. These have no effect on the measured lifetime and therefore no systematic uncertainty is assigned.

5. Results and conclusions

The effective $B_s^0 \to K^+K^-$ lifetime is measured in pp interactions using a data sample corresponding to an integrated luminosity of 1.0 fb^{-1} recorded by the LHCb experiment in 2011. A data-driven approach is used to correct for acceptance effects introduced by the trigger and final event selection. The measurement evaluates the per-event acceptance function directly from the data and determines the effective lifetime to be

$$\tau_{B_s^0 \to K^+K^-} = 1.407 \pm 0.016 \,(\text{stat}) \pm 0.007 \,(\text{syst}) \,\text{ps},$$

which is compatible with the prediction of 1.395 ± 0.020 ps. The measured value is significantly more precise than and supersedes the previous LHCb measurement of this effective lifetime from the same dataset [7], but is statistically independent of the result in Ref. [6]. This measurement can be combined with measurements of $\Delta \Gamma_s$ and Γ_s, given in Ref. [13], to make a first direct determination of the asymmetry parameter $\mathcal{A}_{\Delta \Gamma_s}$ to first order using

$$\mathcal{A}_{\Delta \Gamma_s} = \frac{2\Gamma_s^2}{\Delta \Gamma_s} \tau_{B_s^0 \to K^+K^-} - \frac{2\Gamma_s}{\Delta \Gamma_s}. \tag{6}$$

The value is found to be

$$\mathcal{A}_{\Delta \Gamma_s} = -0.87 \pm 0.17 \,(\text{stat}) \pm 0.13 \,(\text{syst}),$$

which is consistent with the level of CP violation predicted by the SM [8]. In the limit of no CP violation, the effective $B_s^0 \to K^+K^-$ lifetime corresponds to a measurement of Γ_{L} of

$$\Gamma_{\text{L}} = 0.711 \pm 0.008 \,(\text{stat}) \pm 0.004 \,(\text{syst}) \,\text{ps}^{-1}.$$

This is compatible with the value of Γ_{L} determined from the $B_s^0 \to D_s^+ D_s^-$ channel in Ref. [33]. In addition, measurements of the effective $B^0 \to K^+\pi^-$ and $B_s^0 \to \pi^+K^-$ lifetimes are also performed with the same method. The measured effective lifetimes are

$$\tau_{B^0 \to K^+\pi^-} = 1.524 \pm 0.011 \,(\text{stat}) \pm 0.004 \,(\text{syst}) \,\text{ps},$$

$$\tau_{B_s^0 \to \pi^+K^-} = 1.60 \pm 0.06 \,(\text{stat}) \pm 0.01 \,(\text{syst}) \,\text{ps}.$$

The measured B^0 effective lifetime is compatible with the current world average of 1.519 ± 0.007 ps [27], with the effective lifetime of the flavour-specific B_s^0 compatible within 2σ of its respective world average of 1.463 ± 0.032 ps [27].

References

[1] N. Cabibbo, Unitary symmetry and leptonic decays, Phys. Rev. Lett. 10 (1963) 531.

[2] M. Kobayashi, T. Maskawa, *CP* violation in the renormalizable theory of weak interaction, Prog. Theor. Phys. 49 (1973) 652.

[3] LHCb Collaboration, R. Aaij, et al., Measurement of b-hadron branching fractions for two-body decays into charmless charged hadrons, J. High Energy Phys. 10 (2012) 037, arXiv:1206.2794.

[4] LHCb Collaboration, R. Aaij, et al., First evidence of direct *CP* violation in charmless two-body decays of B_s^0 mesons, Phys. Rev. Lett. 108 (2012) 201601, arXiv:1202.6251.

[5] LHCb Collaboration, R. Aaij, et al., First measurement of time-dependent *CP* violation in $B_s^0 \rightarrow K^+ K^-$ decays, J. High Energy Phys. 10 (2013) 183, arXiv:1308.1428.

[6] LHCb Collaboration, R. Aaij, et al., Measurement of the effective $B_s^0 \rightarrow K^+ K^-$ lifetime, Phys. Lett. B 707 (2012) 349, arXiv:1111.0521.

[7] LHCb Collaboration, R. Aaij, et al., Measurement of the effective $B_s^0 \rightarrow K^+ K^-$ lifetime, Phys. Lett. B 716 (2012) 393, arXiv:1207.5993.

[8] R. Fleischer, R. Knegjens, In pursuit of new physics with $B_s^0 \rightarrow K^+ K^-$, Eur. Phys. J. C 71 (2011) 1532, arXiv:1011.1096.

[9] R. Fleischer, $B_{s,d} \rightarrow \pi\pi, \pi K, KK$: status and prospects, Eur. Phys. J. C 52 (2007) 267, arXiv:0705.1121.

[10] Y. Grossman, The B_s^0 width difference beyond the standard model, Phys. Lett. B 380 (1996) 99, arXiv:hep-ph/9603244.

[11] A. Lenz, U. Nierste, Theoretical update of B_s–$\bar{B}_s$ mixing, J. High Energy Phys. 06 (2007) 072, arXiv:hep-ph/0612167.

[12] R. Fleischer, R. Knegjens, Effective lifetimes of B_s decays and their constraints on the B_s^0–$\bar{B}_s^0$ mixing parameters, Eur. Phys. J. C 71 (2011) 1789, arXiv:1109.5115.

[13] LHCb Collaboration, R. Aaij, et al., Measurement of *CP* violation and the B_s^0 meson decay width difference with $B_s^0 \rightarrow J/\psi K^+ K^-$ and $B_s^0 \rightarrow J/\psi \pi^+ \pi^-$ decays, Phys. Rev. D 87 (2013) 112010, arXiv:1304.2600.

[14] LHCb Collaboration, R. Aaij, et al., Measurement of mixing and *CP* violation parameters in two-body charm decays, J. High Energy Phys. 04 (2012) 129, arXiv:1112.4698.

[15] LHCb Collaboration, A.A. Alves Jr., et al., The LHCb detector at the LHC, J. Instrum. 3 (2008) S08005.

[16] R. Aaij, et al., Performance of the LHCb Vertex Locator, arXiv:1405.7808.

[17] M. Adinolfi, et al., Performance of the LHCb RICH detector at the LHC, Eur. Phys. J. C 73 (2013) 24, arXiv:1211.6759.

[18] T. Sjöstrand, S. Mrenna, P. Skands, PYTHIA 6.4 physics and manual, J. High Energy Phys. 05 (2006) 026, arXiv:hep-ph/0603175;
T. Sjöstrand, S. Mrenna, P. Skands, A brief introduction to PYTHIA 8.1, Comput. Phys. Commun. 178 (2008) 852, arXiv:0710.3820.

[19] I. Belyaev, et al., Handling of the generation of primary events in Gauss, the LHCb simulation framework, in: Nuclear Science Symposium Conference Record (NSS/MIC), IEEE, 2010, p. 1155.

[20] D.J. Lange, The EvtGen particle decay simulation package, Nucl. Instrum. Methods A 462 (2001) 152.

[21] P. Golonka, Z. Was, PHOTOS Monte Carlo: a precision tool for QED corrections in Z and W decays, Eur. Phys. J. C 45 (2006) 97, arXiv:hep-ph/0506026.

[22] Geant4 Collaboration, J. Allison, et al., Geant4 developments and applications, IEEE Trans. Nucl. Sci. 53 (2006) 270;
Geant4 Collaboration, S. Agostinelli, et al., Geant4: a simulation toolkit, Nucl. Instrum. Methods A 506 (2003) 250.

[23] M. Clemencic, et al., The LHCb simulation application, Gauss: design, evolution and experience, J. Phys. Conf. Ser. 331 (2011) 032023.

[24] LHCb Collaboration, R. Aaij, et al., Measurement of b-hadron production fractions in 7 TeV pp collisions, Phys. Rev. D 85 (2012) 032008, arXiv:1111.2357.

[25] T. Skwarnicki, A study of the radiative cascade transitions between the Upsilon-prime and Upsilon resonances, PhD thesis, Institute of Nuclear Physics, Krakow, 1986.

[26] M. Pivk, F.R. Le Diberder, sPlots: a statistical tool to unfold data distributions, Nucl. Instrum. Methods Phys. Res., Sect. A 555 (2005) 356, arXiv:physics/0402083.

[27] Particle Data Group, J. Beringer, et al., Review of particle physics, Phys. Rev. D 86 (2012) 010001, and 2013 partial update for the 2014 edition.

[28] K.S. Cranmer, Kernel estimation in high-energy physics, Comput. Phys. Commun. 136 (2001) 198, arXiv:hep-ex/0011057.

[29] M. Pivk, F.R. Le Diberder, sPlot: a statistical tool to unfold data distributions, Nucl. Instrum. Methods A 555 (2005) 356, arXiv:physics/0402083.

[30] LHCb Collaboration, R. Aaij, et al., Measurements of the B^+, B^0, B_s^0 meson and Λ_b^0 baryon lifetimes, J. High Energy Phys. 04 (2014) 114, arXiv:1402.2554.

[31] LHCb Collaboration, R. Aaij, et al., Observation of the decay $B_c^+ \rightarrow B_s^0 \pi^+$, Phys. Rev. Lett. 111 (2013) 181801, arXiv:1308.4544.

[32] K. Hartkorn, H. Moser, A new method of measuring $\Delta\Gamma_s/\Gamma_s$ in the $B_s^0 \bar{B}_s^0$ system, Eur. Phys. J. C 8 (1999) 381.

[33] LHCb Collaboration, R. Aaij, et al., Measurement of the $\bar{B}_s^0 \rightarrow D_s^- D_s^+$ and $\bar{B}_s^0 \rightarrow D^- D_s^+$ effective lifetimes, Phys. Rev. Lett. 112 (2014) 111802, arXiv:1312.1217.

LHCb Collaboration

R. Aaij [41], B. Adeva [37], M. Adinolfi [46], A. Affolder [52], Z. Ajaltouni [5], J. Albrecht [9], F. Alessio [38], M. Alexander [51], S. Ali [41], G. Alkhazov [30], P. Alvarez Cartelle [37], A.A. Alves Jr. [25,38], S. Amato [2], S. Amerio [22], Y. Amhis [7], L. An [3], L. Anderlini [17,g], J. Anderson [40], R. Andreassen [57], M. Andreotti [16,f], J.E. Andrews [58], R.B. Appleby [54], O. Aquines Gutierrez [10], F. Archilli [38], A. Artamonov [35], M. Artuso [59], E. Aslanides [6], G. Auriemma [25,n], M. Baalouch [5], S. Bachmann [11], J.J. Back [48], A. Badalov [36], V. Balagura [31], W. Baldini [16], R.J. Barlow [54], C. Barschel [38], S. Barsuk [7], W. Barter [47], V. Batozskaya [28], Th. Bauer [41], A. Bay [39], J. Beddow [51], F. Bedeschi [23], I. Bediaga [1], S. Belogurov [31], K. Belous [35], I. Belyaev [31], E. Ben-Haim [8], G. Bencivenni [18], S. Benson [38], J. Benton [46], A. Berezhnoy [32], R. Bernet [40], M.-O. Bettler [47], M. van Beuzekom [41], A. Bien [11], S. Bifani [45], T. Bird [54], A. Bizzeti [17,i], P.M. Bjørnstad [54], T. Blake [48], F. Blanc [39], J. Blouw [10], S. Blusk [59], V. Bocci [25], A. Bondar [34], N. Bondar [30,38], W. Bonivento [15,38], S. Borghi [54], A. Borgia [59], M. Borsato [7], T.J.V. Bowcock [52], E. Bowen [40], C. Bozzi [16], T. Brambach [9], J. van den Brand [42], J. Bressieux [39], D. Brett [54], M. Britsch [10], T. Britton [59], N.H. Brook [46], H. Brown [52], A. Bursche [40], G. Busetto [22,q], J. Buytaert [38], S. Cadeddu [15], R. Calabrese [16,f], M. Calvi [20,k], M. Calvo Gomez [36,o], A. Camboni [36], P. Campana [18,38], D. Campora Perez [38], A. Carbone [14,d], G. Carboni [24,l], R. Cardinale [19,38,j], A. Cardini [15], H. Carranza-Mejia [50], L. Carson [50], K. Carvalho Akiba [2], G. Casse [52], L. Cassina [20], L. Castillo Garcia [38], M. Cattaneo [38], Ch. Cauet [9], R. Cenci [58], M. Charles [8], Ph. Charpentier [38], S.-F. Cheung [55], N. Chiapolini [40], M. Chrzaszcz [40,26], K. Ciba [38], X. Cid Vidal [38], G. Ciezarek [53], P.E.L. Clarke [50], M. Clemencic [38], H.V. Cliff [47], J. Closier [38], V. Coco [38], J. Cogan [6], E. Cogneras [5], P. Collins [38], A. Comerma-Montells [11], A. Contu [15,38], A. Cook [46], M. Coombes [46], S. Coquereau [8], G. Corti [38], M. Corvo [16,f], I. Counts [56], B. Couturier [38], G.A. Cowan [50], D.C. Craik [48], M. Cruz Torres [60], S. Cunliffe [53], R. Currie [50], C. D'Ambrosio [38], J. Dalseno [46], P. David [8], P.N.Y. David [41],

A. Davis [57], K. De Bruyn [41], S. De Capua [54], M. De Cian [11], J.M. De Miranda [1], L. De Paula [2], W. De Silva [57], P. De Simone [18], D. Decamp [4], M. Deckenhoff [9], L. Del Buono [8], N. Déléage [4], D. Derkach [55], O. Deschamps [5], F. Dettori [42], A. Di Canto [38], H. Dijkstra [38], S. Donleavy [52], F. Dordei [11], M. Dorigo [39], A. Dosil Suárez [37], D. Dossett [48], A. Dovbnya [43], F. Dupertuis [39], P. Durante [38], R. Dzhelyadin [35], A. Dziurda [26], A. Dzyuba [30], S. Easo [49,38], U. Egede [53], V. Egorychev [31], S. Eidelman [34], S. Eisenhardt [50], U. Eitschberger [9], R. Ekelhof [9], L. Eklund [51,38], I. El Rifai [5], Ch. Elsasser [40], S. Esen [11], A. Falabella [16,f], C. Färber [11], C. Farinelli [41], N. Farley [45], S. Farry [52], R.F. Fay [52], D. Ferguson [50], V. Fernandez Albor [37], F. Ferreira Rodrigues [1], M. Ferro-Luzzi [38], S. Filippov [33], M. Fiore [16,f], M. Fiorini [16,f], M. Firlej [27], C. Fitzpatrick [38], T. Fiutowski [27], M. Fontana [10], F. Fontanelli [19,j], R. Forty [38], O. Francisco [2], M. Frank [38], C. Frei [38], M. Frosini [17,38,g], J. Fu [21,38], E. Furfaro [24,l], A. Gallas Torreira [37], D. Galli [14,d], S. Gallorini [22], S. Gambetta [19,j], M. Gandelman [2], P. Gandini [59], Y. Gao [3], J. Garofoli [59], J. Garra Tico [47], L. Garrido [36], C. Gaspar [38], R. Gauld [55], L. Gavardi [9], A. Geraci [21,u], E. Gersabeck [11], M. Gersabeck [54], T. Gershon [48], Ph. Ghez [4], A. Gianelle [22], S. Giani' [39], V. Gibson [47], L. Giubega [29], V.V. Gligorov [38], C. Göbel [60], D. Golubkov [31], A. Golutvin [53,31,38], A. Gomes [1,a], H. Gordon [38], C. Gotti [20], M. Grabalosa Gándara [5], R. Graciani Diaz [36], L.A. Granado Cardoso [38], E. Graugés [36], G. Graziani [17], A. Grecu [29], E. Greening [55], S. Gregson [47], P. Griffith [45], L. Grillo [11], O. Grünberg [62], B. Gui [59], E. Gushchin [33], Yu. Guz [35,38], T. Gys [38], C. Hadjivasiliou [59], G. Haefeli [39], C. Haen [38], S.C. Haines [47], S. Hall [53], B. Hamilton [58], T. Hampson [46], X. Han [11], S. Hansmann-Menzemer [11], N. Harnew [55], S.T. Harnew [46], J. Harrison [54], T. Hartmann [62], J. He [38], T. Head [38], V. Heijne [41], K. Hennessy [52], P. Henrard [5], L. Henry [8], J.A. Hernando Morata [37], E. van Herwijnen [38], M. Heß [62], A. Hicheur [1], D. Hill [55], M. Hoballah [5], C. Hombach [54], W. Hulsbergen [41], P. Hunt [55], N. Hussain [55], D. Hutchcroft [52], D. Hynds [51], M. Idzik [27], P. Ilten [56], R. Jacobsson [38], A. Jaeger [11], J. Jalocha [55], E. Jans [41], P. Jaton [39], A. Jawahery [58], F. Jing [3], M. John [55], D. Johnson [55], C.R. Jones [47], C. Joram [38], B. Jost [38], N. Jurik [59], M. Kaballo [9], S. Kandybei [43], W. Kanso [6], M. Karacson [38], T.M. Karbach [38], M. Kelsey [59], I.R. Kenyon [45], T. Ketel [42], B. Khanji [20], C. Khurewathanakul [39], S. Klaver [54], O. Kochebina [7], M. Kolpin [11], I. Komarov [39], R.F. Koopman [42], P. Koppenburg [41,38], M. Korolev [32], A. Kozlinskiy [41], L. Kravchuk [33], K. Kreplin [11], M. Kreps [48], G. Krocker [11], P. Krokovny [34], F. Kruse [9], M. Kucharczyk [20,26,38,k], V. Kudryavtsev [34], K. Kurek [28], T. Kvaratskheliya [31], V.N. La Thi [39], D. Lacarrere [38], G. Lafferty [54], A. Lai [15], D. Lambert [50], R.W. Lambert [42], E. Lanciotti [38], G. Lanfranchi [18], C. Langenbruch [38], B. Langhans [38], T. Latham [48], C. Lazzeroni [45], R. Le Gac [6], J. van Leerdam [41], J.-P. Lees [4], R. Lefèvre [5], A. Leflat [32], J. Lefrançois [7], S. Leo [23], O. Leroy [6], T. Lesiak [26], B. Leverington [11], Y. Li [3], M. Liles [52], R. Lindner [38], C. Linn [38], F. Lionetto [40], B. Liu [15], G. Liu [38], S. Lohn [38], I. Longstaff [51], J.H. Lopes [2], N. Lopez-March [39], P. Lowdon [40], H. Lu [3], D. Lucchesi [22,q], H. Luo [50], A. Lupato [22], E. Luppi [16,f], O. Lupton [55], F. Machefert [7], I.V. Machikhiliyan [31], F. Maciuc [29], O. Maev [30], S. Malde [55], G. Manca [15,e], G. Mancinelli [6], A. Mapelli [38], J. Maratas [5], J.F. Marchand [4], U. Marconi [14], C. Marin Benito [36], P. Marino [23,s], R. Märki [39], J. Marks [11], G. Martellotti [25], A. Martens [8], A. Martín Sánchez [7], M. Martinelli [41], D. Martinez Santos [42], F. Martinez Vidal [64], D. Martins Tostes [2], A. Massafferri [1], R. Matev [38], Z. Mathe [38], C. Matteuzzi [20], A. Mazurov [16,f], M. McCann [53], J. McCarthy [45], A. McNab [54], R. McNulty [12], B. McSkelly [52], B. Meadows [57,55], F. Meier [9], M. Meissner [11], M. Merk [41], D.A. Milanes [8], M.-N. Minard [4], N. Moggi [14], J. Molina Rodriguez [60], S. Monteil [5], D. Moran [54], M. Morandin [22], P. Morawski [26], A. Mordà [6], M.J. Morello [23,s], J. Moron [27], R. Mountain [59], F. Muheim [50], K. Müller [40], R. Muresan [29], M. Mussini [14], B. Muster [39], P. Naik [46], T. Nakada [39], R. Nandakumar [49], I. Nasteva [2], M. Needham [50], N. Neri [21], S. Neubert [38], N. Neufeld [38], M. Neuner [11], A.D. Nguyen [39], T.D. Nguyen [39], C. Nguyen-Mau [39,p], M. Nicol [7], V. Niess [5], R. Niet [9], N. Nikitin [32], T. Nikodem [11], A. Novoselov [35], A. Oblakowska-Mucha [27], V. Obraztsov [35], S. Oggero [41], S. Ogilvy [51], O. Okhrimenko [44], R. Oldeman [15,e], G. Onderwater [65], M. Orlandea [29], J.M. Otalora Goicochea [2], P. Owen [53], A. Oyanguren [64], B.K. Pal [59], A. Palano [13,c], F. Palombo [21,t], M. Palutan [18], J. Panman [38], A. Papanestis [49,38], M. Pappagallo [51], C. Parkes [54], C.J. Parkinson [9,45], G. Passaleva [17], G.D. Patel [52], M. Patel [53], C. Patrignani [19,j], A. Pazos Alvarez [37], A. Pearce [54], A. Pellegrino [41], M. Pepe Altarelli [38], S. Perazzini [14,d], E. Perez Trigo [37], P. Perret [5], M. Perrin-Terrin [6], L. Pescatore [45], E. Pesen [66], K. Petridis [53], A. Petrolini [19,j], E. Picatoste Olloqui [36], B. Pietrzyk [4], T. Pilař [48], D. Pinci [25], A. Pistone [19], S. Playfer [50], M. Plo Casasus [37], F. Polci [8], A. Poluektov [48,34], E. Polycarpo [2], A. Popov [35], D. Popov [10], B. Popovici [29], C. Potterat [2], A. Powell [55], J. Prisciandaro [39], A. Pritchard [52], C. Prouve [46], V. Pugatch [44], A. Puig Navarro [39], G. Punzi [23,r], W. Qian [4],

B. Rachwal [26], J.H. Rademacker [46], B. Rakotomiaramanana [39], M. Rama [18], M.S. Rangel [2], I. Raniuk [43],
N. Rauschmayr [38], G. Raven [42], S. Reichert [54], M.M. Reid [48], A.C. dos Reis [1], S. Ricciardi [49], A. Richards [53],
M. Rihl [38], K. Rinnert [52], V. Rives Molina [36], D.A. Roa Romero [5], P. Robbe [7], A.B. Rodrigues [1],
E. Rodrigues [54], P. Rodriguez Perez [54], S. Roiser [38], V. Romanovsky [35], A. Romero Vidal [37], M. Rotondo [22],
J. Rouvinet [39], T. Ruf [38], F. Ruffini [23], H. Ruiz [36], P. Ruiz Valls [64], G. Sabatino [25,l], J.J. Saborido Silva [37],
N. Sagidova [30], P. Sail [51,*], B. Saitta [15,e], V. Salustino Guimaraes [2], C. Sanchez Mayordomo [64],
B. Sanmartin Sedes [37], R. Santacesaria [25], C. Santamarina Rios [37], E. Santovetti [24,l], M. Sapunov [6],
A. Sarti [18,m], C. Satriano [25,n], A. Satta [24], M. Savrie [16,f], D. Savrina [31,32], M. Schiller [42], H. Schindler [38],
M. Schlupp [9], M. Schmelling [10], B. Schmidt [38], O. Schneider [39], A. Schopper [38], M.-H. Schune [7],
R. Schwemmer [38], B. Sciascia [18], A. Sciubba [25], M. Seco [37], A. Semennikov [31], K. Senderowska [27], I. Sepp [53],
N. Serra [40], J. Serrano [6], L. Sestini [22], P. Seyfert [11], M. Shapkin [35], I. Shapoval [16,43,f], Y. Shcheglov [30],
T. Shears [52], L. Shekhtman [34], V. Shevchenko [63], A. Shires [9], R. Silva Coutinho [48], G. Simi [22], M. Sirendi [47],
N. Skidmore [46], T. Skwarnicki [59], N.A. Smith [52], E. Smith [55,49], E. Smith [53], J. Smith [47], M. Smith [54],
H. Snoek [41], M.D. Sokoloff [57], F.J.P. Soler [51], F. Soomro [39], D. Souza [46], B. Souza De Paula [2], B. Spaan [9],
A. Sparkes [50], P. Spradlin [51], F. Stagni [38], S. Stahl [11], O. Steinkamp [40], O. Stenyakin [35], S. Stevenson [55],
S. Stoica [29], S. Stone [59], B. Storaci [40], S. Stracka [23,38], M. Straticiuc [29], U. Straumann [40], R. Stroili [22],
V.K. Subbiah [38], L. Sun [57], W. Sutcliffe [53], K. Swientek [27], S. Swientek [9], V. Syropoulos [42],
M. Szczekowski [28], P. Szczypka [39,38], D. Szilard [2], T. Szumlak [27], S. T'Jampens [4], M. Teklishyn [7],
G. Tellarini [16,f], F. Teubert [38], C. Thomas [55], E. Thomas [38], J. van Tilburg [41], V. Tisserand [4], M. Tobin [39],
S. Tolk [42], L. Tomassetti [16,f], D. Tonelli [38], S. Topp-Joergensen [55], N. Torr [55], E. Tournefier [4], S. Tourneur [39],
M.T. Tran [39], M. Tresch [40], A. Tsaregorodtsev [6], P. Tsopelas [41], N. Tuning [41], M. Ubeda Garcia [38],
A. Ukleja [28], A. Ustyuzhanin [63], U. Uwer [11], V. Vagnoni [14], G. Valenti [14], A. Vallier [7], R. Vazquez Gomez [18],
P. Vazquez Regueiro [37], C. Vázquez Sierra [37], S. Vecchi [16], J.J. Velthuis [46], M. Veltri [17,h], G. Veneziano [39],
M. Vesterinen [11], B. Viaud [7], D. Vieira [2], M. Vieites Diaz [37], X. Vilasis-Cardona [36,o], A. Vollhardt [40],
D. Volyanskyy [10], D. Voong [46], A. Vorobyev [30], V. Vorobyev [34], C. Voß [62], H. Voss [10], J.A. de Vries [41],
R. Waldi [62], C. Wallace [48], R. Wallace [12], J. Walsh [23], S. Wandernoth [11], J. Wang [59], D.R. Ward [47],
N.K. Watson [45], D. Websdale [53], M. Whitehead [48], J. Wicht [38], D. Wiedner [11], G. Wilkinson [55],
M.P. Williams [45], M. Williams [56], F.F. Wilson [49], J. Wimberley [58], J. Wishahi [9], W. Wislicki [28], M. Witek [26],
G. Wormser [7], S.A. Wotton [47], S. Wright [47], S. Wu [3], K. Wyllie [38], Y. Xie [61], Z. Xing [59], Z. Xu [39], Z. Yang [3],
X. Yuan [3], O. Yushchenko [35], M. Zangoli [14], M. Zavertyaev [10,b], F. Zhang [3], L. Zhang [59], W.C. Zhang [12],
Y. Zhang [3], A. Zhelezov [11], A. Zhokhov [31], L. Zhong [3], A. Zvyagin [38]

[1] *Centro Brasileiro de Pesquisas Físicas (CBPF), Rio de Janeiro, Brazil*
[2] *Universidade Federal do Rio de Janeiro (UFRJ), Rio de Janeiro, Brazil*
[3] *Center for High Energy Physics, Tsinghua University, Beijing, China*
[4] *LAPP, Université de Savoie, CNRS/IN2P3, Annecy-Le-Vieux, France*
[5] *Clermont Université, Université Blaise Pascal, CNRS/IN2P3, LPC, Clermont-Ferrand, France*
[6] *CPPM, Aix-Marseille Université, CNRS/IN2P3, Marseille, France*
[7] *LAL, Université Paris-Sud, CNRS/IN2P3, Orsay, France*
[8] *LPNHE, Université Pierre et Marie Curie, Université Paris Diderot, CNRS/IN2P3, Paris, France*
[9] *Fakultät Physik, Technische Universität Dortmund, Dortmund, Germany*
[10] *Max-Planck-Institut für Kernphysik (MPIK), Heidelberg, Germany*
[11] *Physikalisches Institut, Ruprecht-Karls-Universität Heidelberg, Heidelberg, Germany*
[12] *School of Physics, University College Dublin, Dublin, Ireland*
[13] *Sezione INFN di Bari, Bari, Italy*
[14] *Sezione INFN di Bologna, Bologna, Italy*
[15] *Sezione INFN di Cagliari, Cagliari, Italy*
[16] *Sezione INFN di Ferrara, Ferrara, Italy*
[17] *Sezione INFN di Firenze, Firenze, Italy*
[18] *Laboratori Nazionali dell'INFN di Frascati, Frascati, Italy*
[19] *Sezione INFN di Genova, Genova, Italy*
[20] *Sezione INFN di Milano Bicocca, Milano, Italy*
[21] *Sezione INFN di Milano, Milano, Italy*
[22] *Sezione INFN di Padova, Padova, Italy*
[23] *Sezione INFN di Pisa, Pisa, Italy*
[24] *Sezione INFN di Roma Tor Vergata, Roma, Italy*
[25] *Sezione INFN di Roma La Sapienza, Roma, Italy*
[26] *Henryk Niewodniczanski Institute of Nuclear Physics Polish Academy of Sciences, Kraków, Poland*
[27] *AGH – University of Science and Technology, Faculty of Physics and Applied Computer Science, Kraków, Poland*
[28] *National Center for Nuclear Research (NCBJ), Warsaw, Poland*
[29] *Horia Hulubei National Institute of Physics and Nuclear Engineering, Bucharest-Magurele, Romania*
[30] *Petersburg Nuclear Physics Institute (PNPI), Gatchina, Russia*
[31] *Institute of Theoretical and Experimental Physics (ITEP), Moscow, Russia*

[32] Institute of Nuclear Physics, Moscow State University (SINP MSU), Moscow, Russia
[33] Institute for Nuclear Research of the Russian Academy of Sciences (INR RAN), Moscow, Russia
[34] Budker Institute of Nuclear Physics (SB RAS) and Novosibirsk State University, Novosibirsk, Russia
[35] Institute for High Energy Physics (IHEP), Protvino, Russia
[36] Universitat de Barcelona, Barcelona, Spain
[37] Universidad de Santiago de Compostela, Santiago de Compostela, Spain
[38] European Organization for Nuclear Research (CERN), Geneva, Switzerland
[39] Ecole Polytechnique Fédérale de Lausanne (EPFL), Lausanne, Switzerland
[40] Physik-Institut, Universität Zürich, Zürich, Switzerland
[41] Nikhef National Institute for Subatomic Physics, Amsterdam, The Netherlands
[42] Nikhef National Institute for Subatomic Physics and VU University Amsterdam, Amsterdam, The Netherlands
[43] NSC Kharkiv Institute of Physics and Technology (NSC KIPT), Kharkiv, Ukraine
[44] Institute for Nuclear Research of the National Academy of Sciences (KINR), Kyiv, Ukraine
[45] University of Birmingham, Birmingham, United Kingdom
[46] H.H. Wills Physics Laboratory, University of Bristol, Bristol, United Kingdom
[47] Cavendish Laboratory, University of Cambridge, Cambridge, United Kingdom
[48] Department of Physics, University of Warwick, Coventry, United Kingdom
[49] STFC Rutherford Appleton Laboratory, Didcot, United Kingdom
[50] School of Physics and Astronomy, University of Edinburgh, Edinburgh, United Kingdom
[51] School of Physics and Astronomy, University of Glasgow, Glasgow, United Kingdom
[52] Oliver Lodge Laboratory, University of Liverpool, Liverpool, United Kingdom
[53] Imperial College London, London, United Kingdom
[54] School of Physics and Astronomy, University of Manchester, Manchester, United Kingdom
[55] Department of Physics, University of Oxford, Oxford, United Kingdom
[56] Massachusetts Institute of Technology, Cambridge, MA, United States
[57] University of Cincinnati, Cincinnati, OH, United States
[58] University of Maryland, College Park, MD, United States
[59] Syracuse University, Syracuse, NY, United States
[60] Pontifícia Universidade Católica do Rio de Janeiro (PUC-Rio), Rio de Janeiro, Brazil [v]
[61] Institute of Particle Physics, Central China Normal University, Wuhan, Hubei, China [w]
[62] Institut für Physik, Universität Rostock, Rostock, Germany [x]
[63] National Research Centre Kurchatov Institute, Moscow, Russia [y]
[64] Instituto de Fisica Corpuscular (IFIC), Universitat de Valencia-CSIC, Valencia, Spain [z]
[65] KVI – University of Groningen, Groningen, The Netherlands [aa]
[66] Celal Bayar University, Manisa, Turkey [ab]

[*] Corresponding author.
[a] Universidade Federal do Triângulo Mineiro (UFTM), Uberaba-MG, Brazil.
[b] P.N. Lebedev Physical Institute, Russian Academy of Science (LPI RAS), Moscow, Russia.
[c] Università di Bari, Bari, Italy.
[d] Università di Bologna, Bologna, Italy.
[e] Università di Cagliari, Cagliari, Italy.
[f] Università di Ferrara, Ferrara, Italy.
[g] Università di Firenze, Firenze, Italy.
[h] Università di Urbino, Urbino, Italy.
[i] Università di Modena e Reggio Emilia, Modena, Italy.
[j] Università di Genova, Genova, Italy.
[k] Università di Milano Bicocca, Milano, Italy.
[l] Università di Roma Tor Vergata, Roma, Italy.
[m] Università di Roma La Sapienza, Roma, Italy.
[n] Università della Basilicata, Potenza, Italy.
[o] LIFAELS, La Salle, Universitat Ramon Llull, Barcelona, Spain.
[p] Hanoi University of Science, Hanoi, Viet Nam.
[q] Università di Padova, Padova, Italy.
[r] Università di Pisa, Pisa, Italy.
[s] Scuola Normale Superiore, Pisa, Italy.
[t] Università degli Studi di Milano, Milano, Italy.
[u] Politecnico di Milano, Milano, Italy.
[v] Associated to Universidade Federal do Rio de Janeiro (UFRJ), Rio de Janeiro, Brazil.
[w] Associated to Center for High Energy Physics, Tsinghua University, Beijing, China.
[x] Associated to Physikalisches Institut, Ruprecht-Karls-Universität Heidelberg, Heidelberg, Germany.
[y] Associated to Institute of Theoretical and Experimental Physics (ITEP), Moscow, Russia.
[z] Associated to Universitat de Barcelona, Barcelona, Spain.
[aa] Associated to Nikhef National Institute for Subatomic Physics, Amsterdam, The Netherlands.
[ab] Associated to European Organization for Nuclear Research (CERN), Geneva, Switzerland.